



Cite this: *RSC Adv.*, 2018, 8, 19642

Synthesis of polyurethanes with pendant azide groups attached on the soft segments and the surface modification with mPEG by click chemistry for antifouling applications†

Fancui Meng, Zhuangzhuang Qiao, Yan Yao and Jianbin Luo *

Polyurethane with pendant azide groups on the soft segment (PU-GAP) was prepared in this study to further increase the content of reactive azide groups and improve their surfaces enrichment for further functionalization. Polymer diols with pendant azide groups (GAP) were prepared by transforming the pendant chlorine groups at polyepichlorohydrin (PECH) into azide groups with sodium azide. The prepared PECH, GAP and PU-GAP was characterized by GPC, ¹H NMR and FTIR. Propargylic mPEG (mPEG-alkyne) was used as model surface modification reagents which was grafted on the prepared azido containing polyurethane films *via* click chemistry. The surface morphology, chemical composition and wettabilities were studied by SEM, XPS and water contact angle (WCA) analysis, respectively. SEM results demonstrated different surface topologies between mPEG modified PU surface and original PU surface. XPS and WCA analysis proved the successful grafting of mPEG on the pendant azide groups of PUs. The mPEG modified PU surfaces demonstrated good antifouling activities against model bacteria and mPEG with larger molecular weights modified surfaces showed better resistance efficiency to attachment of bacteria. Therefore, the surface reactive polyurethane we prepared can be a universal platform for further functionalization according actual applications.

Received 4th April 2018
 Accepted 23rd May 2018

DOI: 10.1039/c8ra02912a

rsc.li/rsc-advances

1. Introduction

Liner multi-blocked polyurethanes (MPUs)^{1–3} have been widely used in the biomedical field due to their good biocompatibility and excellent mechanical properties. They are a flexible platform of materials that can be designed to fit the requirements for different applications.⁴ Recently, great efforts have been invested in the development of functional polyurethanes for applications.^{5–7} One route to obtain functional polyurethanes is the use of compounds with desirable functionalities and reactive groups, *i.e.* hydroxyl or amine, as a termination for polyurethane prepolymers.^{8–12} However, the low loading capability of the functionalities and the decreased molecular weight of the polyurethanes are two main disadvantages for the chain termination methods. Alternatively, functional groups can be directly introduced into polyurethane hard-segment by using chain extenders with pendant desirable functionalities as a functional building block. Although the loading content of the functionalities is improved compared with chain termination methods, the low surface migration efficiency of the

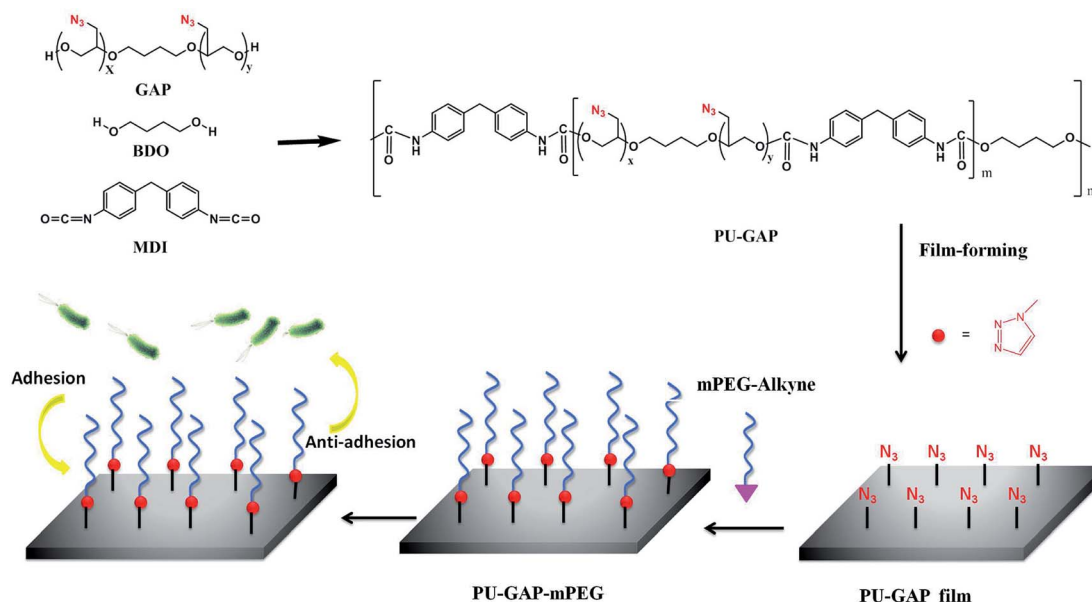
functionalities arising from the low mobility of hard segments results in inefficient surface modification. More recently, alkynyl, azide or cyclic disulfide groups were introduced into hard/soft segments of polyurethanes for further functionalization using click chemistry.^{13–16} Numerous laboratories prepared bioactive modification of biodegradable polyurethane which pendent alkynyl on hard segment and azide-ended peptide were linked to form a 1,2,3-triazole with covalent bonding by click reaction.^{17–20}

Taking into account the surface self-enrichment of soft-segments of PUs as a result of their higher mobility than hard-segments, polyurethane with pendant azide groups on the soft segment (PU-GAP) was prepared firstly in this study to further increase the content of azide groups and improve their surface enrichment.^{21–23} The azide groups on the soft segment afford more reactive agents interacting with antifouling molecules, comparing with the selective modification by the functional groups of the end groups of the polyurethane.²⁴ As one of widely used indwelling biomaterial, polyurethanes with antifouling or/and anti-bacterial activities have been paid close attention all the time due to intense complications caused by bacteria biofilm formation on their surfaces.^{25–27} In order to render biomaterial with antifouling/antibacterial properties, several hydrophilic,^{28,29} hydrophobic,^{30,31} zwitterionic and biocidal agents were grafted onto biomaterial surface.^{32,33}

College of Chemistry and Environmental Protection Engineering, Southwest Minzu University, 610041 Chengdu, China. E-mail: luojb1971@163.com; Tel: +86 28 85522269

† Electronic supplementary information (ESI) available. See DOI: 10.1039/c8ra02912a





Scheme 1 Schematic illustration of structure of the PU-GAP and the surface modification process of PU-GAP film (1.0 cm \times 1.0 cm) with mPEG-alkyne by click chemistry for antifouling applications.

Polyethylene glycol (PEG) has been widely used as antifouling polymer due to its hydrophilic and steric hindrance effect in aqueous medium.^{34,35} Therefore, propargylic mPEG (mPEG-alkyne) was used as model surface modification reagent which was grafted on the prepared azide containing polyurethane film (PU-GAP) *via* click chemistry, resulting PU films with antifouling property. The structure of the PU-GAP and its surface modification process are listed in Scheme 1. It should be mentioned that other bioactive agents with alkyne can be easily grafted onto the prepared polyurethane with pendant azide groups on the soft segment. Therefore, we prepare here a surface reactive polyurethane which can be an universal platform for further functionalization according actual applications.

2. Experimental

2.1 Material

Epichlorohydrin (Dow Chemical, USA), trifluoride diethyl etherate ($\text{BF}_3\text{-OEt}_2$, Tianjin Lianxing Biotechnology Co. Ltd.), 3-bromo-1-propyne (Aladdin, Shanghai), sodium ascorbate (VcNa, Aladdin, Shanghai), trypticase soy agar medium (TSA, AOBOX, Hengshui), trypticase soy liquid medium (TSB, AOBOX, Hengshui), 1,4-butanediol (BDO, KESHI, Chengdu), 4,4'-diphenylmethane diisocyanate (MDI, J&K, Beijing), tetrahydrofuran (THF, Bioway, Shanghai), anhydrous magnesium sulfate (MgSO_4 , Tianjin ZhiYuan Reagent Co. Ltd.), *N,N*-diisopropylethylamine (DIEA, J&K, Beijing) can be used directly. All other chemical reagents such as sodium hydride (NaH), dimethyl sulfoxide (DMSO), sodium azide (NaN_3), methanol, sodium hydroxide (NaOH), diethyl ether, cupric sulfate (CuSO_4), phosphate buffer (PBS), polypropylene glycol (PPG), methylene chloride (DCM) and dimethylformamide (DMF) were purchased

from Sinopharm. *S. aureus* and *E. coli* were purchased from Guangdong Institute of Microbiology. mPEG with number average molecular weights of 5000, 3350 and 1000 (mPEG-5000, mPEG-3350 and mPEG-1000, Aladdin) were used without further purification.

2.2 Synthesis of polyurethane with pendant azide groups

2.2.1 Synthesis of polyepichlorohydrin (PECH). PECH was prepared according to a previously reported method.³⁶ Epichlorohydrin (420 mmol, 38.81 g) was added dropwise to a solution of 1,4-butanediol (20 mmol, 1.80 g) and boron trifluoride diethyl etherate (2 mmol, 250 μL) in DCM (10 mL) at room temperature. After addition of the epichlorohydrin (dropping rate 0.25 mL min^{-1}), the solution was continued to react overnight. The reaction was quenched by the addition of methanol (5 mL). Then the mixture was washed by 5% sodium bicarbonate (10 mL), washed by deionized water until neutral pH, dissolved in DCM and dried by MgSO_4 . Finally, evaporation of the solvent and then vacuum at 10 mm Hg at 90 $^\circ\text{C}$ for 1 h. The yield of PECH was about 92%.

2.2.2 Synthesis of polymer diols with pendant azide groups (GAP). In a three-necked flask, PECH (40 g) solution in DMSO (50 mL) was heated to 95 $^\circ\text{C}$ and NaN_3 (42.2 g) was added in batches. After the addition, another 100 mL DMSO was charged in and the reaction kept for 72 h. After reaction, the reaction mixture and 100 $^\circ\text{C}$ water was completely mixed in equal volume and statically separated. The lower layer was dissolved in 60 mL DCM which was washed with pure water for three times. The organic layer, dried by MgSO_4 for 24 h, was filtered and then concentrated under reduced pressure to yield crude product. GAP was obtained after the crude product was dried *in vacuo* at 90 $^\circ\text{C}$ for 1 h.



2.2.3 Synthesis of polyurethane with pendant azide groups (PU-GAP). A modified two step polymerization process was used to prepare PU-GAP by using GAP as soft segment, MDI and BDO as hard segment. In a 100 mL three-neck flask with a mechanical stirrer, GAP (2.12 mmol, 5 g) were charged in and vacuumed at 90 °C for 2 h. The temperature was reduced to 65 °C and MDI (4.24 mmol, 1.06 g) was added quickly. The prepolymerization process was conducted at 80 °C for 3 h under a dry nitrogen atmosphere in presence of a drop of dibutyltin dilaurate.^{37,38} After the prepolymerization process, the reaction mixture was cooled to 65 °C and BDO (2.12 mmol, 0.19 g) dissolved in 20 mL DMAc was added in. The chain extending reaction was kept at 85 °C for 4 h under a dry nitrogen atmosphere. After that, the mixture was cooled to ambient temperature. Subsequently the crude product was poured into methanol to removing impurities and unreacted moleculars. The precipitant was dissolved in DMAc and casted into PTFE Petri dish which was instantly dried in an vacuum oven at 40 °C, 60 °C and 80 °C for 24 h, respectively, resulting PU-GAP.³⁹

2.3 Surface modification of PU-GAP film by click chemistry

2.3.1 Synthesis of mPEG-alkyne. In a thoroughly dried Schlenk flask, NaH (10 mmol, 0.24 g) was suspended in 100 mL anhydrous DCM, stirring for 30 min. Then 2 mmol mPEG ($M_n = 1000, 3350, \text{ or } 5000$ respectively) was added in and the reaction conducted at 0 °C for 30 min. Subsequently, 3-bromo-1-propyne (15 mmol, 1.78 g) was added drop by drop and the reaction was kept stirring overnight, the reaction temperature was gradually elevated to room temperature naturally. After the reaction, the suspension liquid was filtered and the filtrate was washed with deionized water three times which was subsequently dried with by MgSO_4 for 24 h. MgSO_4 was removed by filtration and the organic phase was concentrated by evaporation and diethyl ether was added in to remove the impurities. The precipitate was dried in vacuum to afford mPEG-alkyne.⁴⁰

2.3.2 Surface modification of PU-GAP film with mPEG-alkyne (PU-GAP-1000, PU-GAP-3350, PU-GAP-5000). In a round-bottom flask, PU-GAP film (1.0 cm \times 1.0 cm) charged with the azide groups (1.80 mmol), mPEG-alkyne (2.70 mmol), the solvent (tertiary butanol and pure water in 1/1 volume ratio), DIEA (18 mmol) and the copper catalyst based on CuI (1.80 mmol) were added into the round-bottom flask one by one. The mixture was stirred for 30 min under the atmosphere of nitrogen. Finally, VcNa (18 mmol) was added. The reaction was performed overnight at room temperature. After that, the film was washed with ammonia and ethyl alcohol. In our work, PU-GAP-1000, PU-GAP-3350, PU-GAP-5000 were prepared from the same method.^{41–44}

2.4 Characterization

FTIR were measured with a Perkin-Elmer (Spectrum 1000) FTIR spectrometer at room temperature.

¹H NMR spectra were obtained with a Varian (Mercury plus-400) NMR spectrometer at room temperature in $\text{DMSO}-d_6$, and chemical shifts were reported in ppm relative to tetramethylsilane (TMS).

Gel permeation chromatography (GPC, Waters 1500-2414, USA) was used to measure the molecular weights and polydispersity index. The mobile phase was THF and the flow rate was 1.00 mL min^{-1} at 40 °C. The molar mass are reported relative to polystyrene (PS) standards.

A JC2000D1 contact angle measuring device (POWER-EACHVR) was used for the water contact angle of all surfaces. The drop volume was 3.0. All samples were taken at room temperature and the values in this paper are the average of seven measurements.

An ESCALAB 250Xi X-ray photoelectron spectrometer (Thermo Scientific company; American), with a monochromatic Al $K\alpha$ X-ray source, was used to analyze the components of different films.

Scanning electron microscope (SEM) images were taken on a field emission scanning electron microscopy (FE-SEM, FEI INSPECT F; America) at 20 kV.

2.5 Bacterial adhesion experiments

2.5.1 Bacterial culture. Two bacterial strains (*S. aureus* and *E. coli*) were used in this experiment. The strains were first grown aerobically for 24 h at 37 °C on agar plates from frozen stocks. The plates can be used for 2 weeks, if kept at 4 °C. The strains were used to make a pre-culture in 10 mL TSB. This pre-culture was incubated at 37 °C for 16 h and used to inoculate a second culture of 100 mL which was incubated for 21 h. Finally, bacteria were suspended in 100 mL of TSB to a concentration of 3×10^8 CFU mL^{-1} .⁴⁵

2.5.2 Bacterial seeding of the membrane and evaluation of bacterial adhesion. In the bacterial adhesion test, membrane samples were cut into small pieces (1.0 cm \times 1.0 cm), and immersed in 1 mL bacterial suspension of 3×10^5 CFU mL^{-1} . After 8 h incubation, the samples were washed with 1 mL PBS (pH = 7.4) twice and were sonicated intermittently with 2 mL PBS (pH = 7.4) while cooling in an ice/water bath for three times 10 s at 30 W. Subsequently, 50 μL diluted the above PBS was used to coat plates. The plates were incubated at 37 °C for 16 h and the number of adhered bacteria was counted.⁴⁶

Live bacterial viability assay was performed by an Olympus FV 1000 laser scanning confocal microscope (Japan). All films were washed one time with 2 mL PBS after 8 h incubation, and then incubated in a 48-well plate with 200 μL of a dyes-containing solution.

3. Results and discussion

3.1 Synthesis of PU-GAP

PECH was synthesized by cationic polymerization of epichlorohydrin using 1,4-butylene glycol and boron trifluoride diethyl ether as initiators at room temperature. The pendant chlorine groups of PECH were transformed into azide groups by sodium azide which resulted in polymer diols with pendant azides (GAP). The GAP was used as polymer diols to prepare polyurethane with pendant azide groups at the soft-segments (PU-GAP). The unimodal GPC curves (Fig. 1) of purified PECH, GAP and PU-GAP confirmed successful polymerization. The



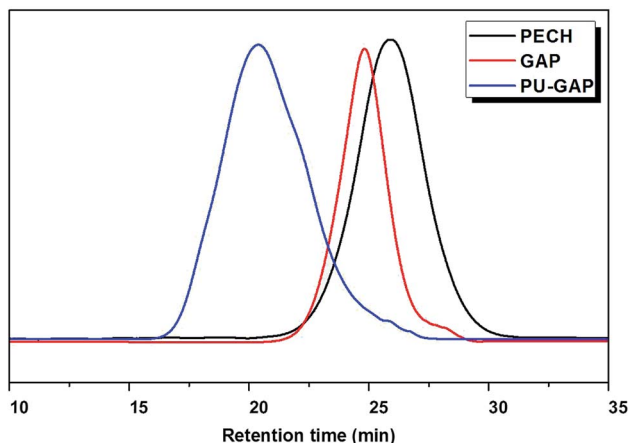


Fig. 1 Representative gel permeation chromatography (GPC) profiles of PECH, GAP and PU-GAP. The shortened retention time is characteristic for a successful increased molecular weight.

Table 1 The average molecular weight and polydispersity of PECH, GAP and PU-GAP

	PECH	GAP	PU-GAP
M_n	2200	2400	29 500
M_w/M_n	1.79	1.93	2.07

average molecular weight and polydispersity of PECH, GAP and PU-GAP are listed in Table 1. By the molar mass of PECH, it was figured out that 1 mol PECH included about 23.78 mol chlorine in theory. When all chlorine was substituted by azide groups to form GAP, the molar mass of GAP should be about 2356. The calculation is consistent with the GPC data. Therefore, it can be sure of that 1 mol GAP contained 23.78 mol azide groups and azide groups on PU-GAP should be 7.93 mmol g^{-1} .

The FTIR spectra of PECH and GAP are shown in Fig. 2. A stretching vibration at 750.5 cm^{-1} corresponding to C-Cl is obviously observed at the spectrum of PECH, which is vanished at the FTIR spectrum of GAP while a characteristic FTIR adsorption of azide groups at 2199.7 cm^{-1} presents at the GAP spectrum. The results preliminarily indicate that C-Cl on PECH was absolutely transformed into azide groups ($-N_3$).

The representative ^1H NMR spectra of PECH, GAP and the assignment of the peaks are presented in Fig. 3. The characteristic resonance of PECH were at 5.37 ppm (hydroxyl protons, $-\text{OH}$), 3.82 ppm (methine, $-\text{CH}-$), 3.62 ppm (methylene, $-\text{CH}-\text{CH}_2-\text{O}-$), 3.57 ppm (methylene, $-\text{CH}-\text{CH}_2-\text{OH}$), 3.37 ppm (methylene, $-\text{CH}-\text{CH}_2-\text{Cl}$), 1.50 ppm (methylene, $-\text{O}-\text{CH}_2-\text{CH}_2-\text{CH}_2-\text{O}-$), respectively. For GAP (Fig. 3), in the ^1H NMR spectra, the appearance of methylene resonance at 3.35 ppm corresponding to methylene protons connected to azide proves the formation of azide, which was also confirmed by ^{13}C NMR spectra (ESI, Fig. S1 †). The formation of mPEG-alkyne was confirmed by ^1H NMR (ESI, Fig. S2 †).

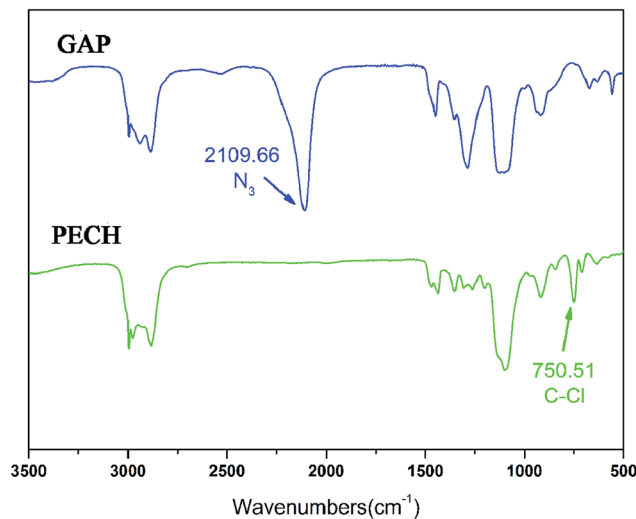


Fig. 2 FTIR spectra of PECH and GAP.

3.2 Surface characterization of PU-GAP film and mPEG modified PU-GAP film

The chemical compositions of the original and modified membranes were analyzed by XPS and the spectra are shown in Fig. 4. Both quantitative and qualitative information on the chemical composition of each element that exists at a depth of several nanometers from the membrane surface can be assessed. The original and modified membranes clearly show major emission peaks at 533 eV for O1s, 401 eV for N1s, and 286 eV for C1s. The surface chemical compositions of the original and modified membranes obtained from XPS results are listed in Table 2. The impurity on the membrane surface was evaluated by considering the C/O ratios. The original PU membrane (PU-GAP) shows a C/O ratio of 4.08. Notable, the C/O ratios of all the mPEG modified films (PU-GAP-1000, PU-GAP-3350, PU-GAP-5000) are nearly 2.0 which suggests the formation of a hydrophilic mPEG layer on the surface of the three

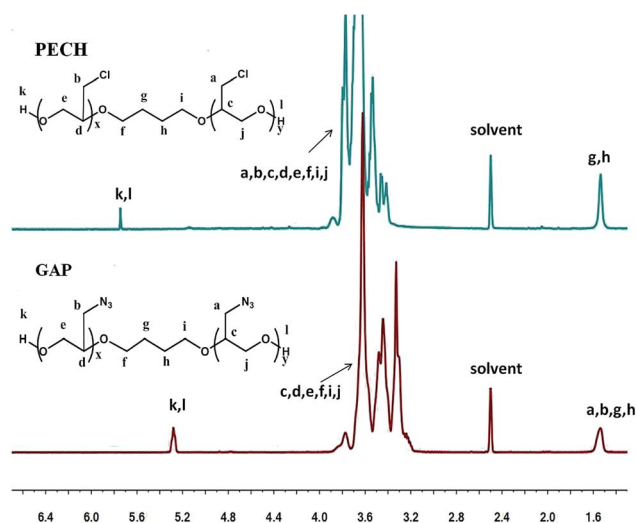


Fig. 3 The ^1H NMR spectra of PECH and GAP.



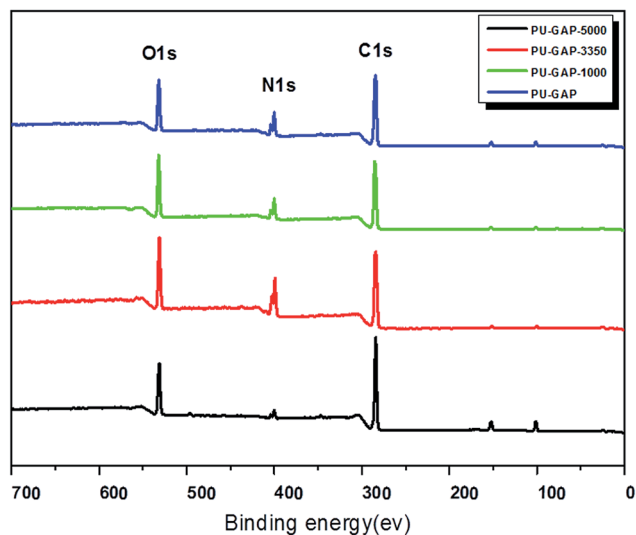


Fig. 4 XPS spectra of the PU-GAP, PU-GAP-1000, PU-GAP-3350, PU-GAP-5000 membranes.

kinds of mPEG modified films. However, the C/O ratios of all the three modified membranes are a little higher than theoretical C/O ratios for mPEG totally covered surfaces with a value of 2.0. The collapse of mPEG chain on the modified surfaces under vacuum atmosphere during XPS detection may account for the higher C/O ratios than theoretical values.

The surface topologies of the original and modified membranes were observed by SEM and the images are presented in Fig. 5. A totally different surface morphologies are found between the modified and unmodified surfaces and among the modified surfaces each other. A typical asymmetric morphology with porous structure was observed in all membranes. The PU-GAP-1000 membrane is smoother than the other two modified membranes, for this reason that the short chain length of mPEG-1000 with good pliability increasing coverage of surface pores. However, structure in PU-GAP-3350 and PU-GAP-5000 membrane surfaces were different from PU-GAP and PU-GAP-1000 membranes. The different porous structures may effect the antifouling activities of membranes. In the previous literatures, the surface of membranes, formed block copolymers or grafted by mPEG, all shown different morphology as a result of variation of the content or molecular weight of mPEG.^{47–50}

It is well known that water contact angle is the most common parameter to evaluate the hydrophilic-hydrophobic property of

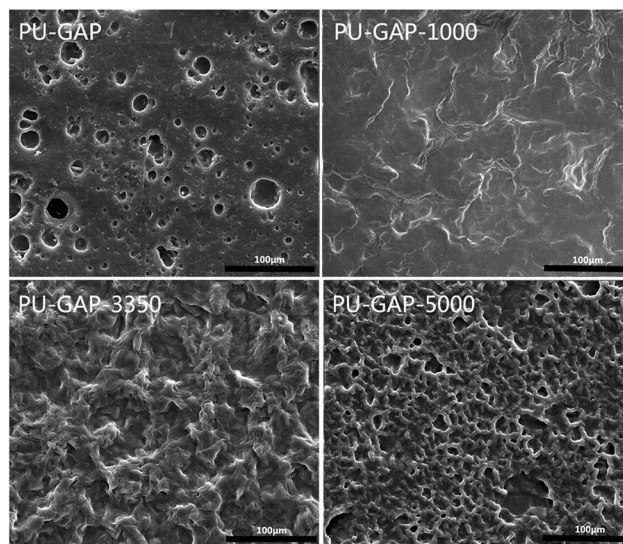


Fig. 5 SEM microphotographs of the surface morphology of unmodified and modified PU membranes.

a membrane surface, especially its antifouling property. Fig. 6A shows the WCA values as a function of time. For original PU-GAP film, the WCA value remains nearly constant (from 120° to 113°) during 1 min contact. However, WCA values of the mPEG modified PU-GAP films present a downward trend, reaching to 72.0°, 8.9° and 47.1° for PU-GAP-1000, PU-GAP-3350 and PU-GAP-5000 respectively after 60 s contact, suggesting the hydrophilic characteristics for these PU films modified by the mPEG chains.^{27,28,33,34} The WCA of PU-GAP-3350 is the lowest after 60 s contact, which may be aroused from their unique surface morphology as shown in Fig. 5.

3.3 Antifouling activities of mPEG modified PU-GAP film

To examine the bacterial adhesion and growth on modified and unmodified original surfaces, a plate count assay was performed after 8 h incubation. A blank PU sample (PU) using PTMG ($M_n = 2000$) instead of GAP as soft segments is used for comparison. The images of *E. coli* and *S. aureus* colonies presenting on agar plates are shown in Fig. 7 and the CFU forming results on the samples are presented in Fig. 8.

As is shown in Fig. 8, a large number of *S. aureus* (8.1×10^5 CFU cm^{-2}) and *E. coli* (4×10^5 CFU cm^{-2}) are found on blank PU surface while partly reduced (for *S. aureus*, 53.9% reduction) or even a little increased (for *E. coli*, 108.5%) of the number of CFUs presents on the PU-GAP surface as comparing with blank PU, suggesting resistance of PU-GAP surface for bacteria adhesion is negligible. However, in comparison with blank PU and PU-GAP, a significant improvement of anti-adhesion activities against both *S. aureus* and *E. coli* are found for the three kinds of mPEG modified surfaces, i.e. PU-GAP-1000, PU-GAP-3350 and PU-GAP-5000. Furthermore, for PU surfaces modified with mPEG of different number-average molecular weight, the antifouling activities against both bacteria strains improve with the increase of chain length of the mPEG. As shown in Fig. 8, PU-GAP-1000, PU-GAP-3350 and PU-GAP-5000 surfaces lead to

Table 2 Surface chemical compositions of the prepared membranes obtained from XPS analysis

Membrane abbreviation	Atom content (%)			C/O
	C	O	N	
PU-GAP	76.3	18.7	5.0	4.1
PU-GAP-1000	68.5	27.4	4.1	2.5
PU-GAP-3350	70.1	26.0	3.9	2.7
PU-GAP-5000	69.2	26.6	4.2	2.6



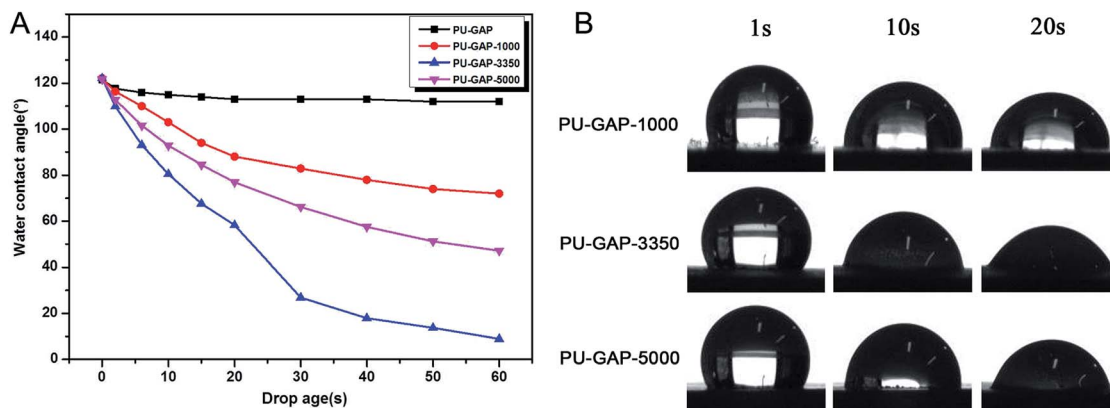


Fig. 6 Water contact angle of PU-GAP, PU-GAP-1000, PU-GAP-3350 and PU-GAP-5000. (A) The water contact angle of the different PU films as a function of time. (B) Water contact image with different state of water drop in films.

a reduction of the number of adhered bacteria for approximately 75–97% relative to PU. The results indicate that the hydrophilic nature and steric hindrance effect of mPEG in

aqueous medium are important to render antifouling performance to the mPEG modified surfaces. In comparison with PU-GAP-1000, the better antifouling efficiency provided by PU-GAP-

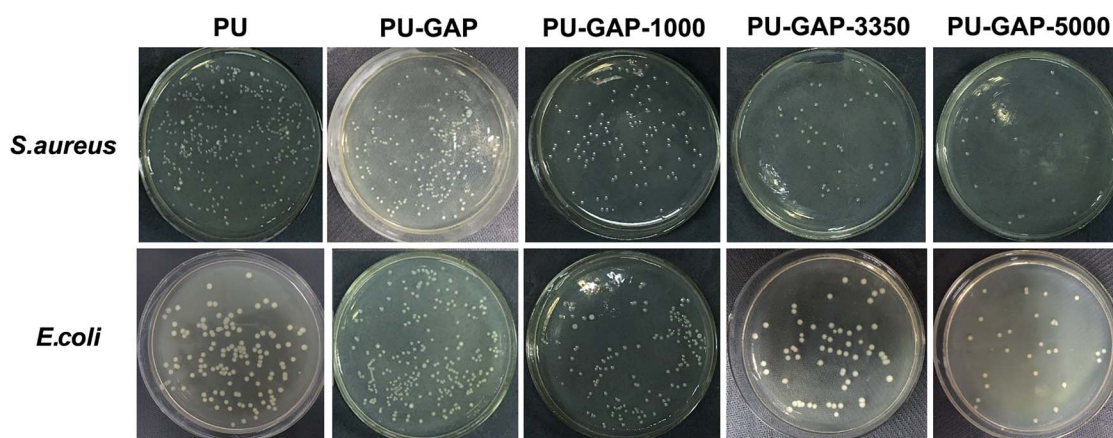


Fig. 7 Digital images of *S. aureus* and *E. coli* colonies on agar plates after 8 h incubation corresponding to the blank control and the original, PU-GAP-1000, PU-GAP-3350 and PU-GAP-5000 films.

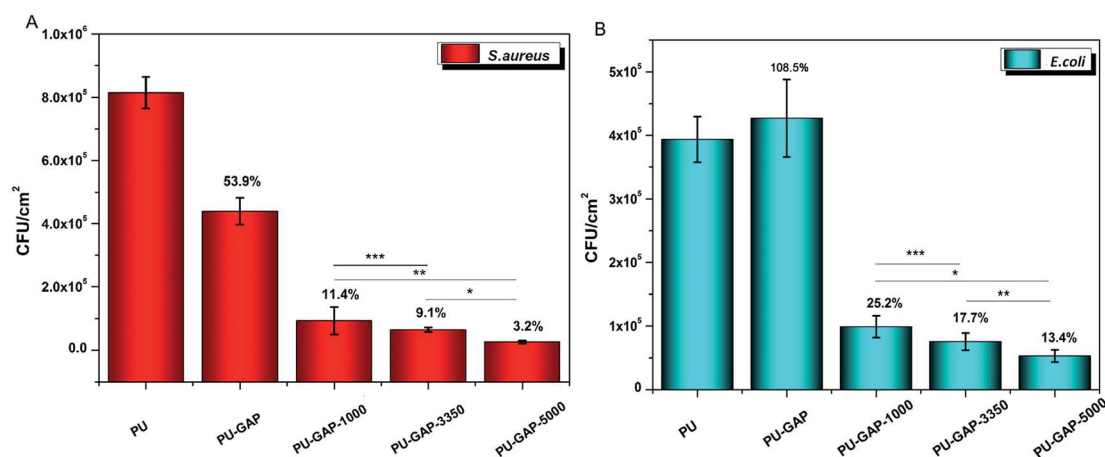


Fig. 8 Antifouling activities of PU, PU-GAP, PU-GAP-1000, PU-GAP-3350, PU-GAP-5000 against *S. aureus* (A) and *E. coli* (B) after 8 h incubation. Statistically significant difference were marked with asterisks (* $P < 0.005$, ** $P < 0.05$, *** $P < 0.5$).



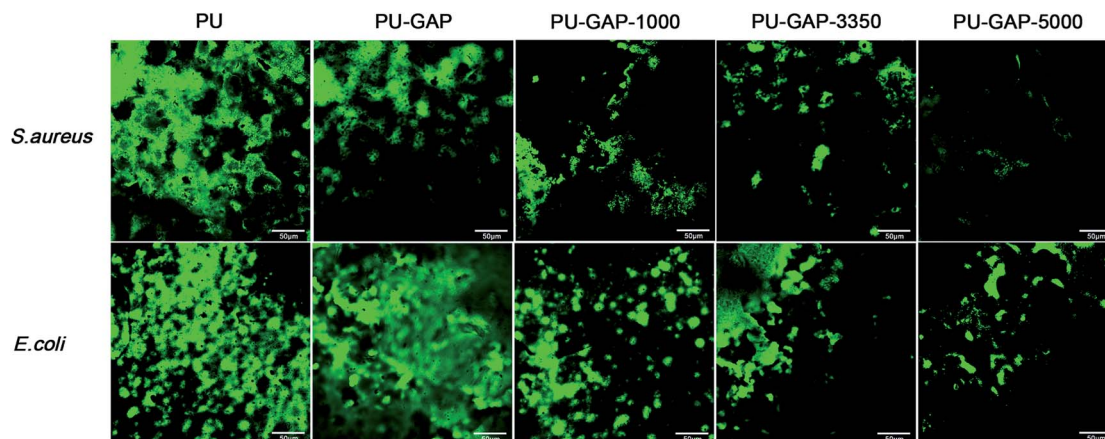


Fig. 9 Confocal microscopy images for different films after 8 h incubation with *E. coli* and *S. aureus*. Both the two strain cells were stained using LIVE/DEAD BacLight Bacterial Viability Kits. Size of the scale bars: 50 μm .

3350 and PU-GAP-5000 is probably due to their enhanced hydrophilic performance as the WCA study has demonstrated.

Laser scanning confocal microscope was used to visually demonstrate the antifouling efficiency of the surfaces modified films after exposure to bacteria suspensions for 8 h and staining the cell membrane intact bacteria (live bacteria) fouled on the surfaces with proprietary cell-permeant nucleic acid stain (SYTO® 9).

As shown in Fig. 9, the PU and PU-GAP surfaces were fully covered by a layer of bacteria consisting of primarily live bacteria. After grafted with mPEG, such as PU-GAP-1000, PU-GAP-3350, PU-GAP-5000, the attachment of both bacteria strains decreased significantly, indicating good antifouling properties of these samples. In addition, PU surfaces modified with higher molecular weight mPEG, *i.e.* PU-GAP-3350, PU-GAP-5000, displayed better resistance to bacteria adhesion.

4. Conclusion

In conclusion, polyurethane with pendant azide groups was synthesized which can be a universal platform for further functionalizing according actual applications by alkynyl-azide click chemistry. mPEG-alkyne was used as an example to modify the PU-GAP surface for antifouling applications. The PU-GAP surface can be easily functionalized with mPEG by click chemistry and the mPEG modified surfaces demonstrated enhanced hydrophilicity and good antifouling activities against two model bacteria.

Conflicts of interest

There are no conflicts to declare.

Acknowledgements

This work was financially supported by the Applied Basic Research Programs Foundation of Sichuan Province (No. 2015JY0126) and by the Functional Polymer Innovation Team Project, Southwest Minzu University (No. 14CXTD04).

References

- 1 I. Francolini, F. Crisante, A. Martinelli, *et al.*, Synthesis of biomimetic segmented polyurethanes as antifouling biomaterials, *Acta Biomater.*, 2012, **8**, 549–558.
- 2 X. Lv, X. Wang, L. Guo, *et al.*, Preparation of PU modified PVDF antifouling membrane and its hydrophilic performance, *J. Membr. Sci.*, 2016, **520**, 933–940.
- 3 S. Rana, S. Y. Lee and J. W. Cho, Synthesis and characterization of biocompatible poly(ethylene glycol)-functionalized polyurethane using click chemistry, *Polym. Bull.*, 2009, **64**(4), 401–411.
- 4 R. Wang, X. Song, T. Xiang, *et al.*, Mussel-inspired chitosan-polyurethane coatings for improving the antifouling and antibacterial properties of polyethersulfone membranes, *Carbohydr. Polym.*, 2017, **168**, 310–319.
- 5 S. Yuan, S. Luan, S. Yan, *et al.*, Facile Fabrication of Lubricant-Infused Wrinkling Surface for Preventing Thrombus Formation and Infection, *ACS Appl. Mater. Interfaces*, 2015, **7**(34), 19466–19473.
- 6 Z. Zhi, Y. Su, Y. Xi, *et al.*, Dual-Functional Polyethylene Glycol-b-polyhexanide Surface Coating with *in vitro* and *in vivo* Antimicrobial and Antifouling Activities, *ACS Appl. Mater. Interfaces*, 2017, **9**, 10383–10397.
- 7 B. R. Knowles, P. Wagner, S. Maclaughlin, *et al.*, Silica Nanoparticles Functionalized with Zwitterionic Sulfobetaine Siloxane for Application as a Versatile Antifouling Coating System, *ACS Appl. Mater. Interfaces*, 2017, **9**, 18584–18594.
- 8 M. Andideh and M. Esfandeh, Effect of surface modification of electrochemically oxidized carbon fibers by grafting hydroxyl and amine functionalized hyperbranched polyurethanes on interlaminar shear strength of epoxy composites, *Carbon*, 2017, **123**, 233–242.
- 9 X. Tian and Y. R. Qiu, 2-methoxyethylacrylate modified polyurethane membrane and its blood compatibility, *Arch. Biochem. Biophys.*, 2017, **631**, 49–57.



- 10 S. Y. Kim, T. H. Lee, Y. I. Park, *et al.*, Influence of material properties on scratch-healing performance of polyacrylate-graft-polyurethane network that undergo thermally reversible crosslinking, *Polymer*, 2017, **128**, 135–146.
- 11 L. Li, X. Ying, J. Liu, *et al.*, Molecularly imprinted polyurethane grafted calcium alginate hydrogel with specific recognition for proteins, *Mater. Lett.*, 2015, **143**, 248–251.
- 12 D. K. Patel, V. Gupta, A. Dwivedi, *et al.*, Superior biomaterials using diamine modified graphene grafted polyurethane, *Polymer*, 2016, **106**, 109–119.
- 13 M. Jia, A. Li, Y. Mu, *et al.*, Synthesis and adhesive property study of polyoxetanes grafted with catechols *via* Cu(I)-catalyzed click chemistry, *Polymer*, 2014, **55**, 1160–1166.
- 14 Z. Li, W. Wu, P. Hu, *et al.*, Click modification of azo-containing polyurethanes through polymer reaction: Convenient, adjustable structure and enhanced nonlinear optical properties, *Dyes Pigm.*, 2009, **81**, 264–272.
- 15 D. Fournier and F. Du Prze, “Click” Chemistry as a Promising Tool for Side-Chain Functionalization of Polyurethanes, *Macromolecules*, 2008, **41**, 4622–4630.
- 16 J. Fang, S. H. Ye, J. Wang, *et al.*, Thiol click modification of cyclic disulfide containing biodegradable polyurethane urea elastomers, *Biomacromolecules*, 2015, **16**, 1622–1633.
- 17 D. Shi, J. Xiao, R. Gu, *et al.*, Polyurethane conjugating TGF- β on surface impacts local inflammation and endoplasmic reticulum stress in skeletal muscle, *J. Biomed. Mater. Res., Part A*, 2017, **105**, 1156–1165.
- 18 J. Xiao, C. Huang, D. Shi, *et al.*, Inflammatory and immunoreactivity in mice induced by intramuscular implants of HSNGLPL peptide grafted-polyurethane, *J. Mater. Chem. B*, 2016, **4**, 1898–1907.
- 19 G. Wu, M. Xiao, J. Xiao, *et al.*, Elastic polyurethane bearing pendant TGF- β 1 affinity peptide for potential tissue engineering applications, *Mater. Sci. Eng., C*, 2018, **83**, 67.
- 20 C. Long, W. Gang, H. Chao, *et al.*, Modification of Polyurethane by “Click” Chemistry, *Chem. J. Chin. Univ.*, 2014, **35**, 853–857.
- 21 S. Kantheti, R. Narayan and K. V. S. N. Raju, Click Chemistry Engineered Hyperbranched Polyurethane-Urea for Functional Coating Applications, *Ind. Eng. Chem. Res.*, 2014, **53**, 8357–8365.
- 22 J. Lafarge, N. Kbir, D. Schapman, *et al.*, Design of self-disinfecting PVC surfaces using the click chemistry, *React. Funct. Polym.*, 2013, **73**, 1464–1472.
- 23 G. Wang, S. Guo and Y. Ding, Synthesis, Morphology, and Properties of Polyurethane-triazoles by Click Chemistry, *Macromol. Chem. Phys.*, 2015, **21**, 1894–1904.
- 24 H. Tao, L. I. Siyue, Y. M. Ng, *et al.*, Self-healing and Bacteria Resistant Coating Materials for Various Substrates, *US Pat.* 15/682,570, 2018-3-1.
- 25 J. W. Costerton, P. Stewart and E. P. Greenber, Bacterial biofilms a common cause of persistent infections, *Science*, 1999, **284**, 1318–1322.
- 26 F. Rivardo, R. J. Turner, G. Allegrone, *et al.*, Anti-adhesion activity of two biosurfactants produced by *Bacillus* spp. prevents biofilm formation of human bacterial pathogens, *Appl. Microbiol. Biotechnol.*, 2009, **83**, 541–553.
- 27 M. R. Nejadnik, H. C. Van Der Mei, W. Norde, *et al.*, Bacterial adhesion and growth on a polymer brush-coating, *Biomaterials*, 2008, **29**, 4117–4121.
- 28 A. Toncheva, R. Mincheva, M. Kancheva, *et al.*, Antibacterial PLA-PEG electrospun fibers: Comparative study between grafting and blending PEG, *Eur. Polym. J.*, 2016, **75**, 223–233.
- 29 W. Jindan, M. Zhengwei and G. Changyou, Controlling the migration behaviors of vascular smooth muscle cells by methoxy poly(ethylene glycol) brushes of different molecular weight and density, *Biomaterials*, 2012, **33**, 810–820.
- 30 D. Xu, Y. Su, L. Zhao, *et al.*, Antibacterial and antifouling properties of a polyurethane surface modified with perfluoroalkyl and silver nanoparticles, *J. Biomed. Mater. Res., Part A*, 2017, **105**, 531–538.
- 31 T. Liu and L. Ye, Synthesis and properties of fluorinated thermoplastic polyurethane elastomer, *J. Fluorine Chem.*, 2010, **131**(1), 36–41.
- 32 W.-W. Yue, H.-J. Li, T. Xiang, *et al.*, Grafting of zwitterion from polysulfone membrane *via* surface-initiated ATRP with enhanced antifouling property and biocompatibility, *J. Membr. Sci.*, 2013, **446**, 79–91.
- 33 X. Chengmei, M. Fanning, Q. Miao, *et al.*, Quantitative fabrication, performance optimization and comparison of PEG and zwitterionic polymer antifouling coatings, *Acta Biomater.*, 2017, **59**, 129–138.
- 34 L. Tiantian, X. Kui, F. Ya, *et al.*, Inducing the migration behavior of endothelial cells by tuning the ligand density on a density-gradient poly(ethylene glycol) surface, *Colloids Surf., B*, 2016, **143**, 557–564.
- 35 K. Pielirowskaa, K. Krol and T. Majka, Polyoxymethylene-copolymer based composites with PEG-grafted hydroxyapatite with improved thermal stability, *Thermochim. Acta*, 2016, **633**, 98–107.
- 36 P. Coneski and M. Schoenfish, Synthesis of nitric oxide-releasing polyurethanes with S-nitrosothiol-containing hard and soft segments, *Polym. Chem.*, 2011, **2**, 906–913.
- 37 Y. Guan, Y. Su, L. Zhao, *et al.*, Biodegradable polyurethane micelles with pH and reduction responsive properties for intracellular drug delivery, *Mater. Sci. Eng., C*, 2017, **75**, 1221–1230.
- 38 C. Liu, Y. Guan, Y. Su, *et al.*, Surface charge switchable and core cross-linked polyurethane micelles as a reduction-triggered drug delivery system for cancer therapy, *RSC Adv.*, 2017, **7**(18), 11021–11029.
- 39 Y. Yao, D. Xu, C. Liu, *et al.*, Biodegradable pH-sensitive polyurethane micelles with different polyethylene glycol (PEG) location for anti-cancer drug carrier applications, *RSC Adv.*, 2016, **6**, 97684–97693.
- 40 J. Eike, W. Jan, N. Sonja, *et al.*, Synthesis of Diacetylene-Containing Peptide Building Blocks and Amphiphiles, Their Self-Assembly and Topochemical Polymerization in Organic Solvents, *Chem.-Eur. J.*, 2009, **15**, 388–404.
- 41 G. Behl, M. Sikka, A. Chhikara, *et al.*, PEG-coumarin based biocompatible self-assembled fluorescent nanoaggregates



- synthesized *via* click reactions and studies of aggregation behavior, *J. Colloid Interface Sci.*, 2014, **416**, 151–160.
- 42 D. Fournier, B. G. De Geest and F. E. Du Prez, On-demand click functionalization of polyurethane films and foams, *Polymer*, 2009, **50**, 5362–5367.
- 43 L.-T. T. Nguyen, J. Devroede, K. Plasschaert, *et al.*, Providing polyurethane foams with functionality: a kinetic comparison of different “click” and coupling reaction pathways, *Polym. Chem.*, 2013, **4**, 1546–1556.
- 44 F. Li, C. Xie, Z. Cheng, *et al.*, Ultrasound responsive block copolymer micelle of poly(ethylene glycol)-poly(propylene glycol) obtained through click reaction, *Ultrason. Sonochem.*, 2016, **30**, 9–17.
- 45 Y. Su, L. Zhao, F. Meng, *et al.*, Silver nanoparticles decorated lipase-sensitive polyurethane micelles for on-demand release of silver nanoparticles, *Colloids Surf., B*, 2017, **152**, 238–244.
- 46 Y. Jiang, Y. Su, L. Zhao, *et al.*, Preparation and antifouling properties of 2-(meth-acryloyloxy)ethyl cholinephosphate based polymers modified surface with different molecular architectures by ATRP, *Colloids Surf., B*, 2017, **156**, 87–94.
- 47 B. Shaojing, J. Zhengguo, L. Xiaoxin, *et al.*, Fabrication of TiO₂ porous thin films using peg templates and chemistry of the process, *Mater. Chem. Phys.*, 2004, **88**, 273–279.
- 48 D. S. Rosa, C. G. F. Guedes and F. Casarin, The effect of the Mw of PEG in PCL/CA blends, *Polym. Test.*, 2004, **24**, 542–548.
- 49 L. Chanaphan and T. Wirach, Coating of porous PVC-PEG membrane with crosslinkable XSBR for O₂/N₂ and CO₂/N₂ separation, *Polymer*, 2016, **96**, 205–212.
- 50 L. Zhang, W. Jihuai, L. Jianming, *et al.*, Influence of molecular weight of PEG on the property of polymer gel electrolyte and performance of quasi-solid-state dye-sensitized solar cells, *Electrochim. Acta*, 2007, **52**, 6673–6678.

